CHAPTER-2

Mononuclear thiocyanate containing nickel(II) and binuclear azido bridged nickel(II) complexes of N_4-coordinate pyrazole based ligand: Syntheses, structures and magnetic properties

- **Paper published:**

  Journal of Molecular Structure, 1050 (2013) 197-203.

Journal of Molecular Structure 1050 (2013) 197–203

Contents lists available at ScienceDirect

Journal of Molecular Structure

journal homepage: www.elsevier.com/locate/molstruc

Mononuclear thiocyanate containing nickel(II) and binuclear azido bridged nickel(II) complexes of N_4-coordinate pyrazole based ligand: Syntheses, structures and magnetic properties

Ankita Solanki [a], Montserrat Monfort [b], Sujit Baran Kumar [a,*]

[a] Department of Chemistry, The Maharaja Sayajirao University of Baroda, Vadodara 390002, India
[b] Departament de Química Inorgànica, Universitat de Barcelona, Martí i Franquès 1-11, 08028 Barcelona, Spain

HIGHLIGHTS

- Synthesis of two mononuclear nickel(II) complexes of the type $[NiL(NCS)_2]$.
- Two new azido bridged dinickel(II) complexes of the type $[Ni_2(L')_2(N_3)_2(\mu\text{-}N_3)_2]$.
- Ligands are tri and tetradentate nitrogen coordinating sites.
- Structure and magnetic properties of the complexes.
- Binuclear complexes show ferromagnetic interaction with J values from 19 to 32 cm^{-1}.

Abstract

Two mononuclear nickel(II) complexes $[Ni(dbdmp)(NCS)_2]$ (**1**) and $[Ni(dbp)(NCS)_2]$ (**2**) and two azido bridged binuclear nickel(II) complexes $[Ni_2(L'_1)_2(N_3)_2(\mu\text{-}N_3)_2]$ (**3**) and $[Ni_2(L'_2)_2(N_3)_2(\mu\text{-}N_3)_2]$ (**4**), where dbdmp, dbp, L'_1 and L'_2 are *N*,*N*-diethyl-*N'*,*N'*-bis((3,5-dimethyl-*1H*-pyrazol-1-yl)methyl)ethane-1,2-diamine (dbdmp), *N*,*N*-bis((*1H*-pyrazol-1-yl)methyl)-*N'*,*N'*-diethylethane-1,2-diamine (dbp), *N*,*N*-diethyl-*N'*-((3,5-dimethyl-*1H*-pyrazol-1-yl)methyl)ethane-1,2-diamine (L'_1) and *N*-((*1H*-pyrazol-1-yl)methyl)-*N'*,*N'*-diethylethane-1,2-diamine (L'_2) have been synthesized and characterized by microanalyses and physico-chemical methods. Single crystal X-ray diffraction analyses revealed that complexes **1** and **2** are mononuclear NCS^- containing Ni(II) complexes with octahedral geometry and complexes **3** and **4** are end-on (μ-1,1) azido bridged binuclear Ni(II) complexes with distorted octahedral geometry. Variable temperature magnetic studies of the complexes **3** and **4** display ferromagnetic interaction with *J* values 19 and 32 cm^{-1}, respectively.

2.1. Introduction

The pseudohalides like NCS^- and N_3^- are ambidentate ligands that can coordinate to metal ions in different modes. In addition to their monodentate behavior and formation of corresponding mononuclear complexes, the two ions can act as bridging ligand and form di- or polynuclear complexes. Generally, the azide ion displays more bridging modes in polynuclear transition metal complexes in comparison to thiocyanate ion and it can bind metal ions either in the end-to-end (μ-1,3) or in the end-on (μ-1,1) modes [1-29]. A wide range of magnetic behaviours are observed when azide ion binds to transition metal complexes in the different coordination modes. Normally, the end-to-end (μ-1,3) mode of the azido bridge shows antiferromagnetic (AF) interaction and the end-on (μ-1,1) mode produces ferromagnetic (F) coupling. Moreover, the magnitude of magnetic exchange depends on the metal-metal separation, the dihedral angle between the planes containing the metal ion and the metal bridging ligand bond lengths.

The study of coordination chemistry of transition metal complexes with pyrazole based ligands have been of significant interest as they are involved in bioactivities [30-31]. The azido bridged binuclear nickel complexes have received more attention in the area of research owing to the magnetic interactions as well as development of magnetic materials [32–36].

In the present chapter, we report on the syntheses, characterization, structure and magnetic studies of two new tetradentate ligands *N*,*N*-diethyl-*N'*,*N'*-bis((3,5-dimethyl-*1H*-pyrazol-1-yl)methyl)ethane-1,2-diamine (dbdmp), *N*,*N*-bis((*1H*-pyrazol-1-yl)methyl)-*N'*,*N'*-diethylethane-1,2-diamine (dbp) and their NCS^- containing nickel(II) complexes $[Ni(dbdmp)(NCS)_2]$ (**1**) and $[Ni(dbp)(NCS)_2]$ (**2**) and two new azido bridged binuclear nickel(II) complexes $[Ni_2(L'_1)_2(N_3)_2(\mu\text{-}N_3)_2]$ (**3**) and $[Ni_2(L'_2)_2(N_3)_2(\mu\text{-}N_3)_2]$ (**4**), where L'_1 and L'_2 are *N*,*N*-diethyl-*N'*-((3,5-dimethyl-*1H*-pyrazol-1-yl)methyl) ethane-1,2-diamine (L'_1) and *N*-((*1H*-pyrazol-1-yl)methyl)-*N'*,*N'*-diethylethane-1,2-diamine (L'_2). The ligands L'_1 and L'_2 are produced from ligands dbdmp and dbp, respectively during reaction.

2.2. Experimental

2.2.1. Materials

The chemicals and solvents were of analytical grade and purchased from commercial sources. Acetyl acetone (GR, Loba, India), paraformaldehyde (GR, Loba, India), hydrazine hydrate (GR, Loba, India), KSCN, NaN_3 (Qualigens, India), *N*,*N*-diethylethylenediamine (Aldrich), pyrazole (Aldrich), CH_3CN (AR, Merck) were of reagent grade and used as received. $Ni(ClO_4)_2.6H_2O$ was prepared by reaction of nickel carbonate with dilute $HClO_4$ acid and followed by slow evaporation of the solution**.** 1-hydroxymethyl-3,5-dimethylpyrazole and 1-hydroxymethylpyrazole was synthesized according to the reported method [37].

2.2.2. Syntheses of Ligands

2.2.2.1. Synthesis of *N*,*N*-diethyl-*N′*,*N′*-bis((3,5-dimethyl-1H-pyrazol-1-yl) methyl)ethane-1,2-diamine (dbdmp)

To a stirring solution of *N*,*N*-diethylethylenediamine (0.232 g, 2 mmol) in acetonitrile (10 ml), 1-hydroxymethyl-3,5-dimethylpyrazole (0.504 g, 4 mmol) in acetonitrile (10 ml) was added drop by drop. This mixture was stirred at 80º C for 72 h and dried over anhydrous sodium sulphate. The solvent was removed on a vacuum rotary evaporator and finally the compound was obtained as yellow liquid. Yield. 0.53 g (80 %). IR (Neat) cm^{-1}; ν(C_2H_5 +CH_3), 2969 s, 2929 s, 2872 s, 2808 s; ν(C = C) + ν (C = N)/pz ring, 1555 s, 1459 s; ^{1}H NMR (400 MHz, $CDCl_3$, 20°C), *δ*/ppm: 0.919-0.955 (t, 6H, -CH_2-CH_3), 2.188-2.194 (s, 12H, 4 -CH_3 of pz), 2.312-2.349 (t, 2H, -CH_2 of ethylenediamine), 2.397-2.432(q, 4H, -CH_2-CH_3), 2.734-2.771 (t, 2H, -CH_2 of ethylenediamine), 4.918 (s, 4H, N-CH_2-N), 5.822 (s, 2H, -CH of pz ring). ^{13}C NMR (400 MHz, $CDCl_3$, 20 °C), *δ*/ppm: 10.86, 11.40, 13.41, 46.84, 47.03, 50.45, 65.70, 105.75, 139.60 and 147.43.

2.2.2.2. *N*,*N*-bis((*1H*-pyrazol-1-yl)methyl)-*N′*,*N′*-diethylethane-1,2-diamine (dbp)

This compound was synthesized using 1-hydroxymethylpyrazole (4 mmol) instead of 1-hydroxymethyl-3,5-dimethylpyrazole following an analogous procedure to that mentioned for ligand dbdmp. Yield. 0.370 g (78 %). IR (Neat) cm^{-1}; ν(C = C) + ν (C = N)/pz ring, 1559 s, 1458 s; ν(C_2H_5 +CH_3), 2951 s, 2920 s, 2864 s; ^{1}H NMR

(400 MHz, $CDCl_3$, 20 °C), *δ*/ppm: 0.989-1.025 (t, 6H, $-CH_2-CH_3$), 2.312-2.349 (t, 2H, $-CH_2$ of ethylenediamine), 2.490-2.571(q, 6H, $-CH_2-CH_3$ and $-CH_2$ of ethylenediamine), 2.799-2.833 (t, 2H, $-CH_2$ of ethylenediamine), 5.079 (s, 4H, $N-CH_2-N$), 6.294 (s, 2H, -CH of pz ring), 7.558-7.624 (dd, 2H, $-CH_2$ of pz ring). ^{13}C NMR (400 MHz, $CDCl_3$, 20 °C), *δ*/ppm: 11.38, 46.96, 47.80, 51.01, 68.03, 105.91, 129.84 and 139.65.

2.2.3. Syntheses of Complexes

2.2.3.1. [Ni(dbdmp)$(NCS)_2$] (1)

To a methanol solution of $Ni(ClO_4)_2.6H_2O$ (0.183 g, 0.5 mmol) was added a solution of ligand dbdmp (0.166 g, 0.5 mmol) in methanol. The colour of the solution changed to green immediately. Finally, an aqueous solution of KSCN (0.097 g, 1 mmol) was added slowly to the resulting solution. The resulting blue solution was stirred for 2-3 h at room temperature. Slow evaporation of the solution yielded blue coloured needle shape crystals. Yield. 0.190 g (75 %). Found C = 47.69, H = 6.69, N = 22.43 %. Anal calc for $C_{20}H_{32}N_8NiS_2$: C = 47.35, H = 6.36, N = 22.09 %. IR (KBr pellet) cm^{-1}; ν(NCS^-), 2100 vs; ν(C_2H_5 +CH_3), 2972 s, 2925 s, 2869 s; ν(C = C) + ν (C = N)/pz ring, 1554 s, 1466 s. UV-Vis spectra: λ_{max}/nm (ε_{max}/$mol^{-1}cm^{-1}$). 673 (17), 418 (36), 339 (471). μ_{eff} = 2.89 BM.

2.2.3.2. [Ni(dbp)$(NCS)_2$] (2)

This compound was prepared following an analogous procedure to that mentioned above for **1** using ligand dbp. Yield. 0.140 g (62 %). Found C = 42.39, H = 5.30, N = 24.63 %. Anal calc for $C_{16}H_{24}N_8NiS_2$: C = 42.59, H = 5.36, N = 24.83 %. IR (KBr pellet) cm^{-1}; ν(NCS^-), 2098 vs; ν(C_2H_5 +CH_3), 3098, 2980 s, 2940 s, 2881 s; ν(C = C) + ν (C = N)/pz ring, 1518 s, 1470 s. UV-Vis spectra: λ_{max}/nm (ε_{max}/$mol^{-1}cm^{-1}$). 672 (21), 418 (35), 340 (435). μ_{eff} = 2.88 BM.

Caution! Transition metal complex with azide ion and organic ligands are potentially explosive. Only a small amount of material should be synthesized and it should be handled with care.

2.2.3.3. $[Ni_2(L'_1)_2(N_3)_2(\mu\text{-}N_3)_2]$ (3)

To a methanol solution of $Ni(ClO_4).6H_2O$ (0.185 g, 0.5 mmol) was added ligand dbdmp (0.166 g, 0.5 mmol) in methanol (10 ml). The colour of the solution was changed to green immediately. Finally, an aqueous solution of NaN_3 (0.065 g, 1 mmol) was added in to the solution and resulting light green solution was stirred for 3 h at room temperature. Slow evaporation of the solution yielded a light green colored crystal after five days. Yield. 0.100 g (54 %). Found C = 39.38, H = 6.65, N = 38.33 %. Anal calc for $C_{24}H_{48}N_{20}Ni_2$: C = 39.25, H = 6.54, N = 38.16 %. IR (KBr pellet) cm^{-1}; $\nu(N_3^-)$, 2061 vs; ν(NH), 3183 vs; ν(C = C) + ν (C = N)/pz ring, 1553 s, 1468 s.

2.2.3.4. $[Ni_2(L'_2)_2(N_3)_2(\mu\text{-}N_3)_2]$ (4)

This compound was prepared following an analogous procedure to that mentioned above for **3** using ligand dbp. Yield. 0.087 g (51%). Found C = 35.38, H = 5.83, N = 41.39 %. Anal calc for $C_{20}H_{40}N_{20}Ni_2$: C = 35.41, H = 5.90, N = 41.31 %. IR (KBr pellet) cm^{-1}; ν(NH), 3233 vs; $\nu(N_3^-)$, 2042 vs; ν(C = C) + ν(C = N)/pz ring, 1560 s, 1464 s.

2.2.4. Physical Measurements

The IR spectra were recorded on a Perkin-Elmer FT-IR spectrometer RX1 spectrum using KBr pellets. The micro analyses (C, H and N) were carried out using a Perkin-Elmer IA 2400 series elemental analyzer. ^1H and ^{13}C NMR spectra were recorded on Bruker NMR AV400 spectrometer in $CDCl_3$. UV-Vis spectra (900 - 190 nm) were recorded on a Perkin-Elmer spectrophotometer model Lambda 35 in acetonitrile solution. Solution conductivity were measured in acetonitrile solution (10^{-3} M) using Equip-Tronics conductivity meter (model no. EQ-660A). Room temperature magnetic susceptibilities of powder samples were measured using a Faraday magnetic balance equipped with a Mettler UMX 5 balance, OMEGA temperature controller with a field strength of 0.8 Tesla using $Hg[Co(SCN)_4]$ as the reference.

Variable temperature magnetic measurements were carried out in the “Servei de Magnetoquímica (Universitat de Barcelona)” on polycrystalline samples (30 mg) with a Quantum Design SQUID MPMS-XL magnetometer working in the 2-300 K range. The magnetic field was 0.1 *T*. The diamagnetic corrections were evaluated from Pascal’s constants.

2.3. X-ray Crystallography

The crystallographic data, details of data collection and some important features of the refinement for the compounds **1**, **2**, **3** and **4** are given in Table 2.1. Selected bond lengths and angles are given in Table 2.2. Crystals of suitable size of complexes **1, 2, 3** and **4** were obtained by slow evaporation of methanol solution. Data were collected with Mo-K_α radiation (λ = 0.71073Å) at 110 K for complex **1**and **3** and at 293 K for complex **4** respectively, on a Bruker SMART APEX diffractometer equipped with CCD area detector. For complex **2** Data were collected with Cu-K_α radiation (λ = 1.54184Å) at 293 K on Oxford X-CALIBUR-S CCD diffractometer. The data interpretation were processed with SAINT software [38] and empirical absorption correction was applied with SADABS [39] software programs. All structures were solved by direct methods using SHELXTL [40] and refined by the full-matrix least-square based on F^2 technique using SHELXL-97 [41] program package. All non-hydrogen atoms were refined anisotropically. The positions of the hydrogen atoms were calculated from the difference Fourier map.

Table 2.1. Crystal parameters of complexes **1, 2, 3** and **4**.

	[Ni(dbdmp)(NCS)$_2$]	**[Ni(dbp)(NCS)$_2$]**	**[Ni$_2$(L'$_1$)$_2$(N$_3$)$_2$(μ-N$_3$)$_2$]**	**[Ni$_2$(L'$_2$)$_2$(N$_3$)$_2$(μ-N$_3$)$_2$]**
	(1)	**(2)**	**(3)**	**(4)**
Empirical formula	$C_{20}H_{32}N_8NiS_2$	$C_{16}H_{24}N_8Ni_1S_2$	$C_{24}H_{48}N_{20}Ni_2$	$C_{20}H_{40}N_{20}Ni_2$
Formula weight	507.37	451.26	734.20	678.10
Temperature (K)	110(2)	293(2)	110(2)	293(2)
Wavelength (Å)	0.71073	1.54184	0.71073	0.71073
Crystal system	Monoclinic	Monoclinic	Monoclinic	Monoclinic
Space group	*P2$_1$*/C	*P2$_1$*/n	*P2$_1$*/n	*P2$_1$*/C
a (Å)	13.739(3)	13.324(3)	9.3897(7)	8.8057(4)
b (Å)	9.8884(19)	11.249(3)	14.5969(11)	12.2656(6)
c (Å)	19.492(4)	14.836(5)	12.3030(10)	13.9102(7)
~(°)	90	90	90	90
(°)	110.198(3)	110.02(3)	97.1590(10)	96.2220(10)
¥(°)	90	90	90	90
Volume (Å^3)	2485.3(8)	2089.3(10)	1673.1(2)	1493.55(12)
Z	4	4	2	2
Density (gm/m^3)	1.356	1.311	1.457	1.508

Absorption coefficient (mm^{-1})	0.972	0.783	1.176	1.309
F(000)	1072	864	776	716
θ range for data collection (°)	1.58 to 25.00	3.85 to 71.91	2.17 to 28.15	2.22 to 24.36
Index ranges	$-11 \le h \le 16$,	$-16 \le h \le 14$,	$-12 \le h \le 9$,	$-10 \le h \le 10$,
	$-8 \le k \le 11$,	$-13 \le k \le 13$,	$-7 \le k \le 19$,	$-14 \le k \le 14$,
	$-23 \le l \le 23$	$-18 \le l \le 15$	$-16 \le l \le 15$	$-16 \le l \le 16$
Reflections collected	9917	6007	8274	13261
Independent reflections	4350 [R_{int} = 0.0286]	3636 [R_{int} = 0.0413]	3789 [R_{int} = 0.0172]	2443 [R_{int} = 0.0407]
Max. and min. transmission	0.8293 and 0.6526	1.0000 and 0.37060	0.8162 and 0.5199	0.7970 and 0.6478
Data / restraints / parameters	4350 / 0 / 308	3636 / 0 / 245	3789 / 0 / 216	2443 / 0 / 196
Goodness-of-fit on F^2	1.103	1.244	1.053	0.801
Final *R* indices [$I > 2\sigma(I)$]	*R1* = 0.0636,	*R1* = 0.0713,	*R1* = 0.0267,	*R1* = 0.0291,
	wR2 = 0.1389	*wR2* = 0.2030	w*R2* = 0.0688	w*R2* = 0.0923
R indices (all data)	*R1* = 0.0701,	*R1* = 0.1102,	*R1* = 0.0282,	*R1* = 0.0379,
	wR2 = 0.1425	*wR2* = 0.2926	w*R2* = 0.0696	w*R2* = 0.1046
Largest diff. peak and hole (eA^{-3})	0.554 and -0.750	1.247 and -1.335	0.402 and -0.469	0.215 and -0.303
CCDC	895758	946791	895759	917544

Table 2.2. Bond lengths (Å) and bond angles (˚) of Complexes **1, 2, 3** and **4**.

Bond Lengths (Å)							
[Ni(dbdmp)(NCS)$_2$] (1)		**[Ni(dbp)(NCS)$_2$] (2)**		**[Ni$_2$(L'$_1$)$_2$(N$_3$)$_2$(μ-N$_3$)$_2$] (3)**		**[Ni$_2$(L'$_2$)$_2$(N$_3$)$_2$(μ-N$_3$)$_2$] (4)**	
Ni(1) – N(7)	1.992(4)	Ni(1) – N(7)	2.079(6)	Ni(1) – N(5)	2.0670(13)	Ni(1) – N(5)	2.069(2)
Ni(1) – N(8)	2.052(4)	Ni(1) – N(8)	1.968(6)	Ni(1) – N(1)	2.0756(12)	Ni(1) – N(1)	2.068(2)
Ni(1) – N(5)	2.090(4)	Ni(1) – N(5)	2.060(7)	Ni(1) – N(8)	2.0964(12)	Ni(1) – N(8)	2.087(2)
Ni(1) – N(1)	2.103(4)	Ni(1) – N(1)	2.096(7)	Ni(1) – N(3)	2.1115(12)	Ni(1) – N(3)	2.125(2)
Ni(1) – N(3)	2.144(3)	Ni(1) – N(3)	2.137(6)	Ni(1) – N(8)	2.1598(12)	Ni(1) – N(8)	2.192(2)
Ni(1) – N(6)	2.260(4)	Ni(1) – N(6)	2.250(6)	Ni(1) – N(4)	2.2068(12)	Ni(1) – N(4)	2.228(2)
				Ni(1)---Ni(1)	3.2362(3)	Ni(1)---Ni(1)	3.2394(4)
Bond Angles (º)							
N(1) – Ni(1) – N(3)	78.55(14)	N(1) – Ni(1) – N(3)	78.7(3)	N(5) – Ni(1) – N(1)	99.74(5)	N(5) – Ni(1) – N(1)	98.27(9)
N(7) – Ni(1) – N(6)	99.28(16)	N(7) – Ni(1) – N(6)	173.3(3)	N(5) – Ni(1) – N(8)	89.18(5)	N(5) – Ni(1) – N(8)	89.32(10)
N(8) – Ni(1) – N(6)	90.96(17)	N(8) – Ni(1) – N(6)	94.1(2)	N(1) – Ni(1) – N(8)	163.75(5)	N(1) – Ni(1) – N(8)	165.19(9)
N(5) – Ni(1) – N(6)	89.65(18)	N(5) – Ni(1) – N(6)	89.4(2)	N(5) – Ni(1) – N(3)	175.01(5)	N(5) – Ni(1) – N(3)	177.21(9)
N(7) – Ni(1) – N(8)	90.32(18)	N(7) – Ni(1) – N(8)	92.4(3)	N(1) – Ni(1) – N(3)	80.80(5)	N(1) – Ni(1) – N(3)	80.16(9)
N(7) – Ni(1) – N(5)	97.26(18)	N(7) – Ni(1) – N(5)	87.7(3)	N(8) – Ni(1) – N(3)	89.16(5)	N(8) – Ni(1) – N(3)	91.71(10)
N(8) – Ni(1) – N(5)	172.20(15)	N(8) – Ni(1) – N(5)	100.2(3)	N(5) – Ni(1) – N(8)	87.47(5)	N(5) – Ni(1) – N(8)	89.12(9)
N(7) – Ni(1) – N(1)	99.07(15)	N(7) – Ni(1) – N(1)	87.2(3)	N(1) – Ni(1) – N(8)	85.80(5)	N(1) – Ni(1) – N(8)	85.76(8)
N(8) – Ni(1) – N(1)	87.48(14)	N(8) – Ni(1) – N(1)	101.3(3)	N(8) – Ni(1) – N(8)	81.02(5)	N(8) – Ni(1) – N(8)	81.64(9)
N(5) – Ni(1) – N(1)	89.48(16)	N(5) – Ni(1) – N(1)	158.1(3)	N(3) – Ni(1) – N(8)	87.63(5)	N(3) – Ni(1) – N(8)	88.46(9)
N(7) – Ni(1) – N(3)	176.88(16)	N(7) – Ni(1) – N(3)	90.5(2)	N(5) – Ni(1) – N(4)	101.35(5)	N(5) – Ni(1) – N(4)	99.23(9)
N(8) – Ni(1) – N(3)	91.59(15)	N(8) – Ni(1) – N(3)	177.1(2)	N(1) – Ni(1) – N(4)	92.66(4)	N(1) – Ni(1) – N(4)	91.56(9)
N(5) – Ni(1) – N(3)	80.76(14)	N(5) – Ni(1) – N(3)	80.1(2)	N(8) – Ni(1) – N(4)	98.91(5)	N(8) – Ni(1) – N(4)	99.79(8)
N(1) – Ni(1) – N(6)	161.59(14)	N(1) – Ni(1) – N(6)	93.2(2)	N(3) – Ni(1) – N(4)	83.55(5)	N(3) – Ni(1) – N(4)	83.15(9)
N(3) – Ni(1) – N(6)	83.16(15)	N(3) – Ni(1) – N(6)	82.9(2)	N(8) – Ni(1) – N(4)	171.18(5)	N(8) – Ni(1) – N(4)	171.53(8)

2.4. Results and Discussion

2.4.1. Syntheses

The ligands *N*,*N*-diethyl-*N'*,*N'*-bis((3,5-dimethyl-1H-pyrazol-1-yl) methyl) ethane-1,2-diamine (dbdmp) and *N*,*N*-bis((*1H*-pyrazol-1-yl)methyl)-*N'*,*N'*-diethyl ethane-1,2-diamine (dbp) were synthesized by condensation of two equivalents of 1-hydroxymethyl-3,5-dimethylpyrazole or 1-hydroxymethylpyrazole and one equivalent of *N*,*N*-diethylethylenediamine for three days at 80ºC in acetonitrile [scheme 2.1]. The ligands were obtained as viscous liquid with excellent yield (80 %) and characterized by various spectroscopic techniques like IR, ^{1}H and ^{13}C NMR spectroscopy. The ligands are tetradentate with N_4-coordination sites.

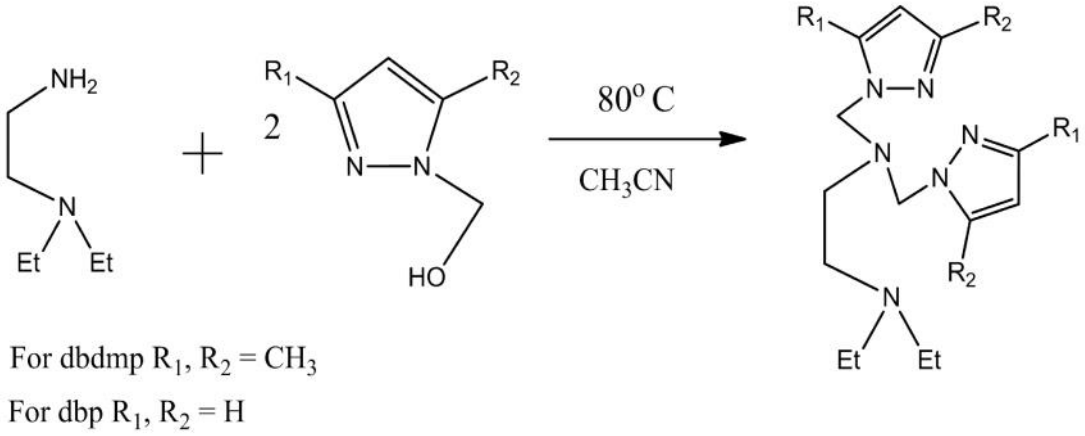

Scheme 2.1. Syntheses of ligands dbdmp and dbp.

Mononuclear octahedral complexes **1** and **2** were synthesized by the reaction of $Ni(ClO_4)_2.6H_2O$, ligand dbdmp or dbp and NCS^- ion in 1:1:2 mole ratio in methanol at room temperature [Scheme 2.2]. Coordination behavior of the ligands and geometry of the complexes **1** and **2** were obtained from crystal structure determination of the complexes [Fig.2.1]. When the same reactions were carried out with 1:1:1 of metal, ligand and thiocyanate ion, we always obtained sticky mass. We are also unable to isolate any product with NCO^- ion under the same reaction condition. The elemental analyses are consistent with the formula of the complexes. Both the complexes are soluble in common organic solvents like methanol, dichloromethane and acetonitrile.

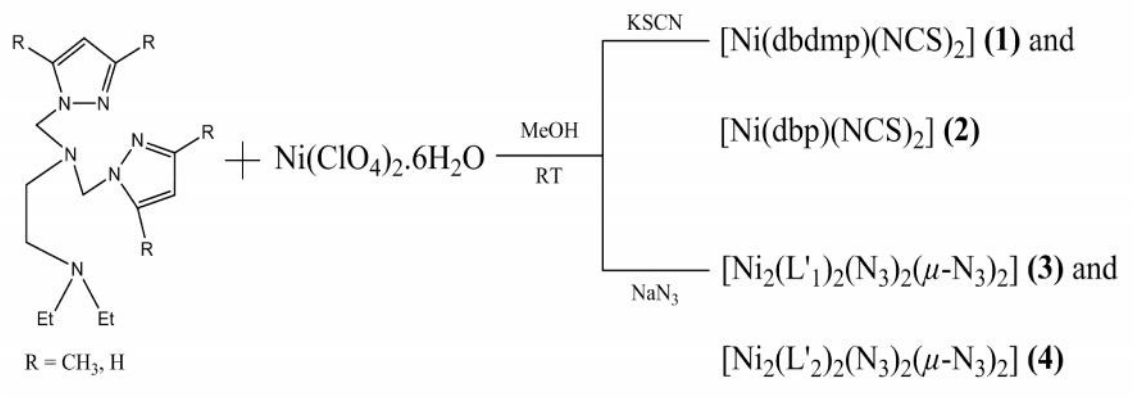

Scheme 2.2. Syntheses of complexes.

The azido bridged binuclear Ni(II) complexes **3** and **4** were synthesized by the reaction of $Ni(ClO_4)_2.6H_2O$, ligand dbdmp/dbp and N_3^- ion in 1:1:2 mole ratio in methanol at room temperature [Scheme 2.2]. The important point of the reaction was that both the tetradentate N_4-coordinated ligands dbdmp and dbp were transformed into tridentate N_3-coordinated L_1' and L_2' respectively, during reaction medium with the removal of pyrazole ring and double end-on azido bridged octahedral complexes were always formed [Scheme 2.3]. This was proved by single crystal X-ray diffraction studies.

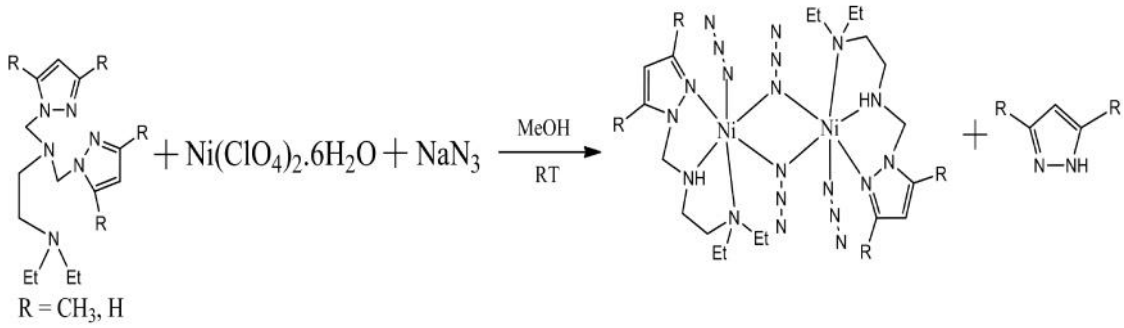

Scheme 2.3. Syntheses of complexes **3** and **4**.

As ligands were same for both NCS^- and N_3^- containing complexes and transformation of ligands had taken place in the azide complexes only, it can be assumed that additional azide ion in presence of methanol was responsible for removal of pyrazole. Similar type of ligand transformations with pyrazole based ligands are already reported in the literature [42-45]. When ligand and azide ion were added to nickel salt in presence of methanol, octahedral nickel(II) complex was formed - the

three coordination sites, two sites by two end-on bridged and one by terminal, were occupied by azide ions and remaining three coordination sites occupied by three nitrogen atoms of the ligand, leaving one uncoordinated arm in the ligand. The pendant arm of tetradentate ligand was removed by cleaving two C-N bonds i.e. N(pyrazole)-CH_2 and CH_2–N(amine) of the N(pyrazole)-CH_2–N(amine) arm and the ligands were transformed into tridentate N_3-coordinated ligands through the mechanism involving metal-mediated cleavage of the pyrazole nitrogen-carbon bond [44]. Isolation of pyrazole molecule from solution further supported our evidence. The probable reasons of the cleaving are the followings. (i) The energy required to break NH_2-CH_2 bond is lower than CH_2-pyrazole bond in NH_2-CH_2-pyrazole arm. (ii). Due to tautomerism,

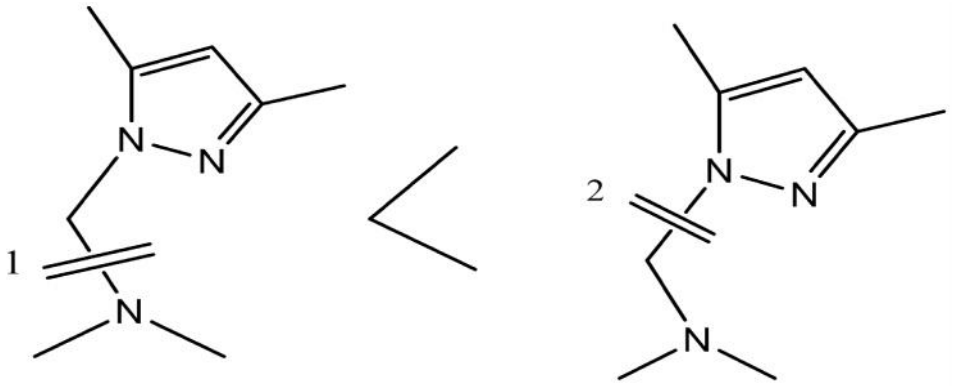

the proton on the nitrogen atom of the pyrazole ring interchange its position between the two nitrogen and bond attached with amine nitrogen with methyl-pyrazole arm become unstable [45].

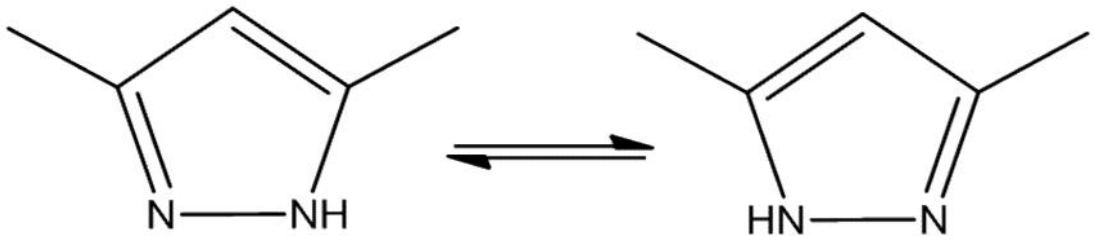

Another important aspect is that when this reaction was carried out in 1:1:1 mole ratio of $Ni(ClO_4)_2.6H_2O$, ligand dbdmp/dbp and NaN_3, unstable compound were formed.

In the study reported here, the present N_4-coordinated tetradentate *N*,*N*-diethylethylenediamine based pyrazole containing ligand form double end-on (μ-1,1) azido bridged complexes with the loss of pyrazole arm and coordination of an additional azide ion. In comparison, tetradentate N_4-coordinated pyridylpyrazole based ligand form double end-to-end (μ-1,3) azide bridged complex without losing any pyrazole arm [46] and with no additional coordination of azide ion. Since the difference between the two ligands were the coordination of pyridine nitrogen or nitrogen from *N*,*N*-diethylethylenediamine, different coordination mode of the azide ions in the two complexes may be due to different steric effect of the two ligands and additional coordination of azide ion.

2.4.2. Description of Crystal Structures

2.4.2.1. [Ni(dbdmp)$(NCS)_2$] (1) and [Ni(dbp)$(NCS)_2$] (2)

An ORTEP view with coordination atmosphere of the mononuclear complexes **1** and **2** are shown in the Fig.2.1. Selected bond lengths and angles related to the metal coordination sphere for the structure are given in Table 2.2. For both the complexes, the coordination sphere around the nickel (II) center can be described as distorted octahedral, having a NiN_6 chromophore, comprises of four nitrogen atoms from ligand dbdmp/dbp – two pyrazole ring nitrogen atoms N(1) and N(5), two tertiary amine nitrogen atoms N(3) and N(6) and two terminal nitrogen atoms N(7) and N(8) from two thiocyanate ions.

For the complex **1**, the equatorial positions are occupied by the four nitrogen atoms N(3), N(5), N(7) and N(8) while axial positions are occupied by N(1) and N(6). The bond distances in the equatorial planes Ni–N(3), Ni–N(5), Ni–N(7), Ni(1)–N(8) are 2.144(4) Å, 2.090(4) Å, 1.992(4) Å and 2.052(4) Å, respectively. The axial bond lengths Ni–N(1) and Ni–N(6) are 2.103(4) Å and 2.250(4) Å, respectively. The bond angles N(8)–Ni(1)–N(5), N(7)–Ni(1)–N(3) and N(1)–Ni(1)–N(6) are 172.20(15)º, 176.88(16)º and 161.59(14)º, respectively.

For the complex **2**, the equatorial positions are occupied by the four nitrogen atoms N(3), N(6), N(7) and N(8), while axial positions are occupied by N(1) and N(5). The distances of four equatorial bonds Ni–N(3), Ni–N(6), Ni–N(7), Ni(1)–N(8) are 2.137(6) Å, 2.250(6) Å, 2.079(6) Å and 1.968(6) Å, respectively. The axial bond

lengths Ni–N(1) and Ni–N(5) are 2.096(7) Å and 2.060(7) Å, respectively and both are equal to each other. The bond angles N(3)–Ni(1)–N(8), N(6)–Ni(1)–N(7) and N(1)–Ni(1)–N(5) are 177.1(2)º, 173.3(3)º and 158.1(3)º, respectively.

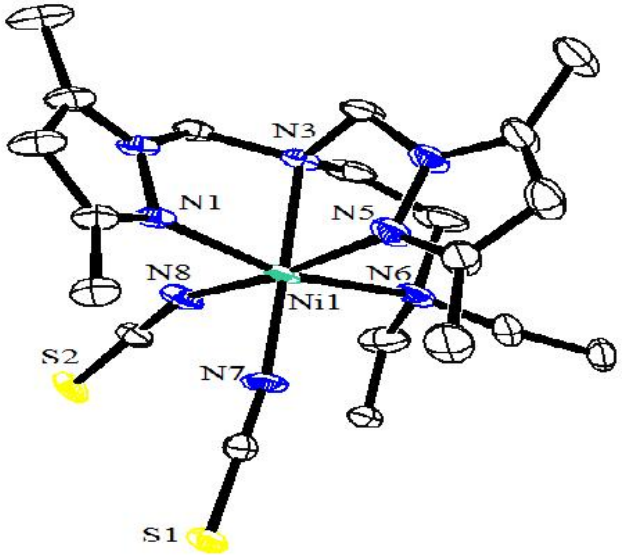

(a) $[Ni(dbdmp)(NCS)_2]$ **(1)**

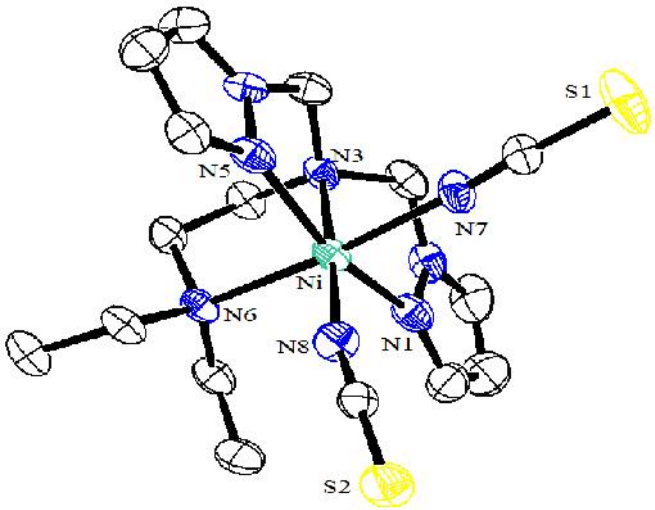

(b) $[Ni(dbp)(NCS)_2]$ **(2)**

Fig.2.1. ORTEP diagram of the complexes (a) $[Ni(dbdmp)(NCS)_2]$ **(1)** and (b) $[Ni(dbp)(NCS)_2]$ **(2)** (30% probability factor for the thermal ellipsoids, H-atoms are omitted for clarity).

2.4.2.2. $[Ni_2(L'_1)_2(N_3)_2(\mu\text{-}N_3)_2]$ (3) and $[Ni_2(L'_2)_2(N_3)_2(\mu\text{-}N_3)_2]$ (4)

The molecular structures of the binuclear moiety of complexes **3** and **4** with coordination atmosphere are shown in Fig.2.2.

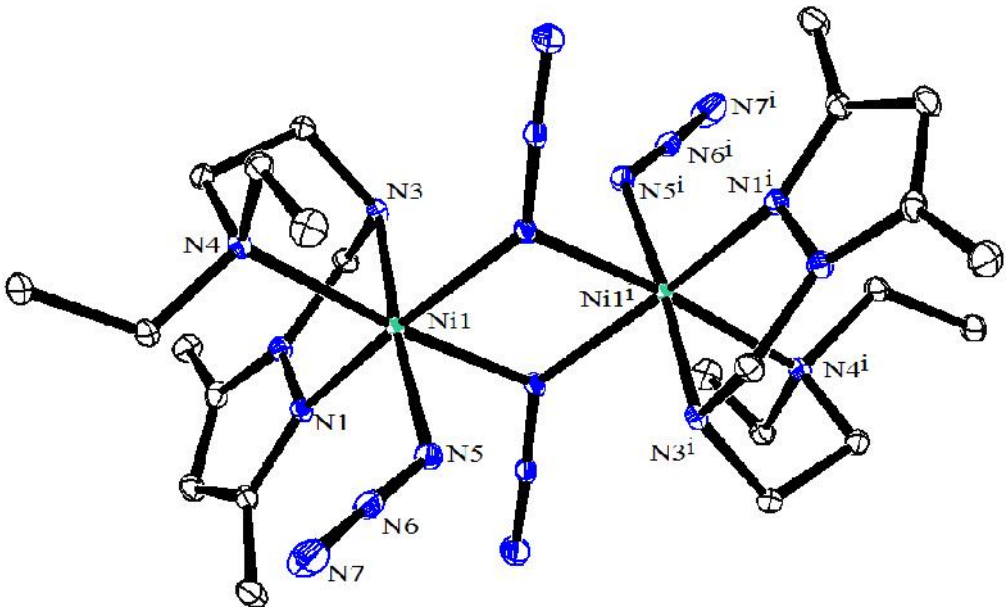

(a) $[Ni_2(L'_1)_2(N_3)_2(\mu\text{-}N_3)_2]$ **(3)**

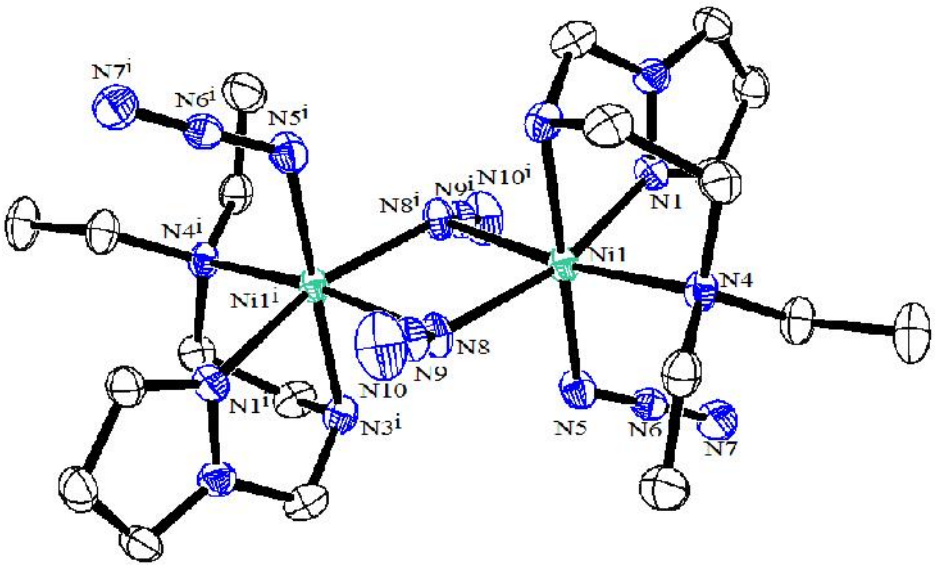

(b) $[Ni_2(L'_2)_2(N_3)_2(\mu\text{-}N_3)_2]$ **(4)**

Fig.2.2. ORTEP diagram of the dimeric complexes (a) $[Ni_2(L'_1)_2(N_3)_2(\mu\text{-}N_3)_2]$ **(3)** and (b) $[Ni_2(L'_2)_2(N_3)_2(\mu\text{-}N_3)_2]$ **(4)** with atom numbering scheme (30% probability for the thermal ellipsoids, H-atoms are omitted for clarity).

The complexes **3** and **4** are crystallized in $P2_1/n$ and $P2_1/C$ space group respectively with two molecules per unit cell. In both cases each half of binuclear complexes, the tridentate ligand L'_1 or L'_2 is ligated facially and the other sites are occupied by one terminal and two bridging azide group. In the distorted NiN_6 octahedral environment, each nickel atom is six coordinated and bounded to four nitrogen atoms - one pyrazole ring's nitrogen N(1), one tertiary amine's nitrogen N(4) and two bridging azide's nitrogen atoms N(8) and N(8a) at the basal position-plus one secondary amine N(3) and one terminal azide's nitrogen N(5) at the axial positions. The distances between two nickel centers Ni(1)----Ni(1) is 3.2362(3) and 3.2394(4) Å for complexes **3** and **4,** respectively and they are equal. The angle of terminal azido group N-N-N is 178.10° for **3** and 178.6° for **4** and the corresponding angle of μ-$_{1,1}$ bridging azido is 178.31° for **3** and 177.9° for **4**. For complex **3**, the distances of four equatorial bonds Ni(1)–N(1), Ni(1)–N(4), Ni(1)–N(8) and Ni(1)–N(8a) are 2.0756(12) Å, 2.2068(12) Å, 2.1598(12) Å and 2.0964(12) Å, respectively. The axial bond lengths Ni(1)–N(3) [2.1115(12) Å] and Ni(1)–N(5) [2.0670(13) Å] are almost same and the N(8)–Ni(1)–N(8a) angle is 81.02(5) Å. The bond angles Ni(1)–N(8)–Ni(1), N(8a)–Ni(1)–N(4), N(8)–Ni(1)–N(4), N(9)–N(8)–Ni(1) and N(9)–N(8a)–Ni(1) are 98.98(5)°, 98.91(5)°, 171.18(5)°, 115.75(9)° and 135.84(10)°, respectively.

For complex **4**, in the equatorial plane, the bond distances of Ni(1)–N(1), Ni(1)–N(4), Ni(1)–N(8) and Ni(1)–N(8a) are 2.068(2) Å, 2.228(2) Å, 2.192(2) Å, 2.087(2) Å and axial bond lengths Ni(1)–N(3), Ni(1)–N(5) are 2.125(2) and 2.069(2) Å, respectively. The bond angles Ni(1)–N(8)–Ni(1), N(8a)–Ni(1)–N(4), N(8)–Ni(1)–N(4), N(9)–N(8)–Ni(1) and N(9)–N(8a)–Ni(1) are 98.36(9)°, 171.53(8)°, 99.79(8)°, 115.37(18)° and 130.28(19)º, respectively.

2.4.3. Spectral Data and Magnetic Susceptibility

2.4.3.1. IR Spectra

The IR spectra of free ligands show strong bands in the region 2969-2808 cm^{-1} indicates the presence of alkyl group. IR spectra of ligands and complexes **1-4** show two strong bands at 1560 and 1455 cm^{-1} indicating the presence of pyrazole group. A sharp band at ~3235 cm^{-1} for complexes **3** and **4** and absence of same band for complexes **1** and **2** indicate the presence of –NH group which were generated during the complex formation. The strong absorption band at 2100 and 2098 cm^{-1} for

complexes **1** and **2** due to NCS^- and at 2061 and 2042 cm^{-1} for complexes **3** and **4** respectively due to N_3^- ion confirm the coordination of the respective group in the complexes. The ligands and all complexes show one strong band at 1576 cm^{-1} indicating the presence of ν(C=N) (azomethine) group in the complexes. All other bands of ligands are also observed in the complexes.

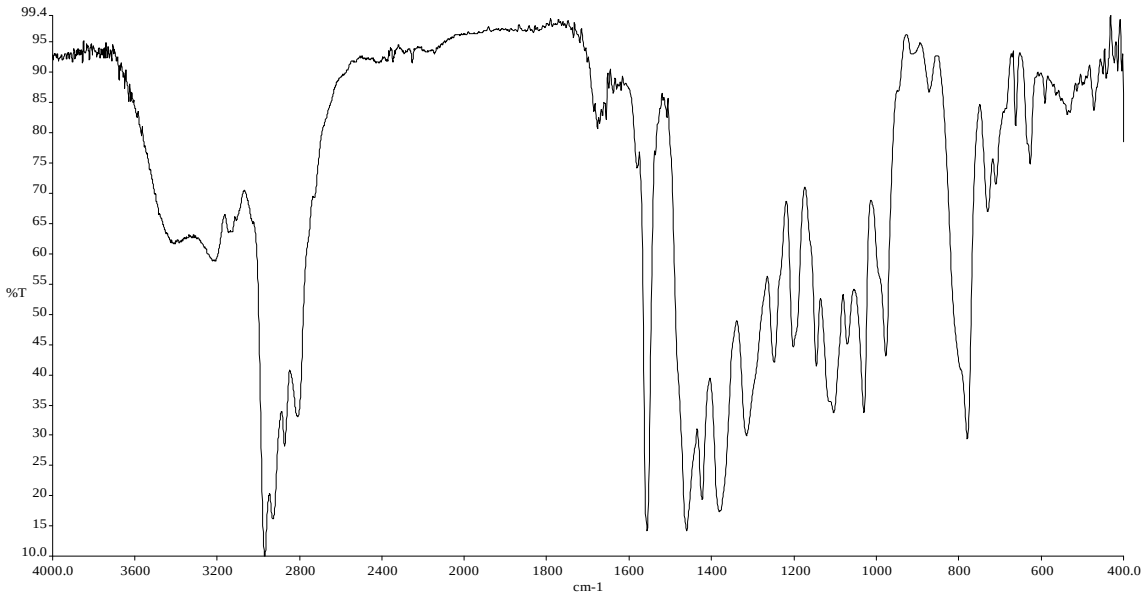

Fig.2.3. IR spectrum of ligand *N*,*N*-diethyl-*N′*,*N′*-bis((3,5-dimethyl-*1H*-pyrazol-1-yl)methyl)ethane-1,2-diamine (dbdmp).

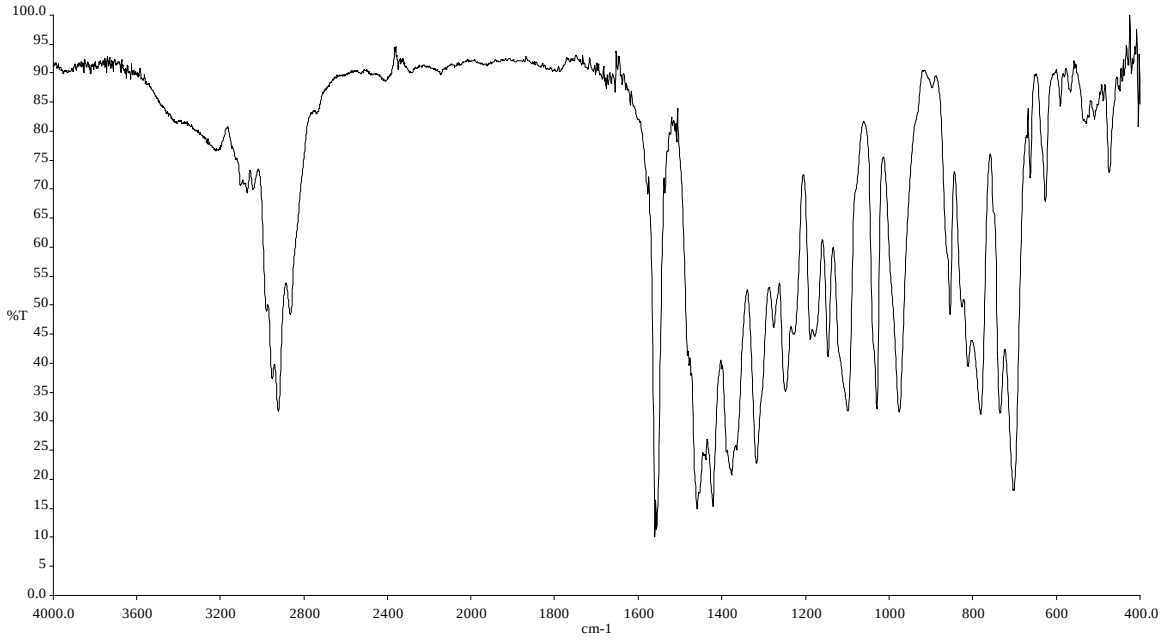

Fig.2.4. IR spectrum of ligand *N*,*N*-bis((*1H*-pyrazol-1-yl)methyl)-*N′*,*N′*-diethyl ethane-1,2-diamine (dbp).

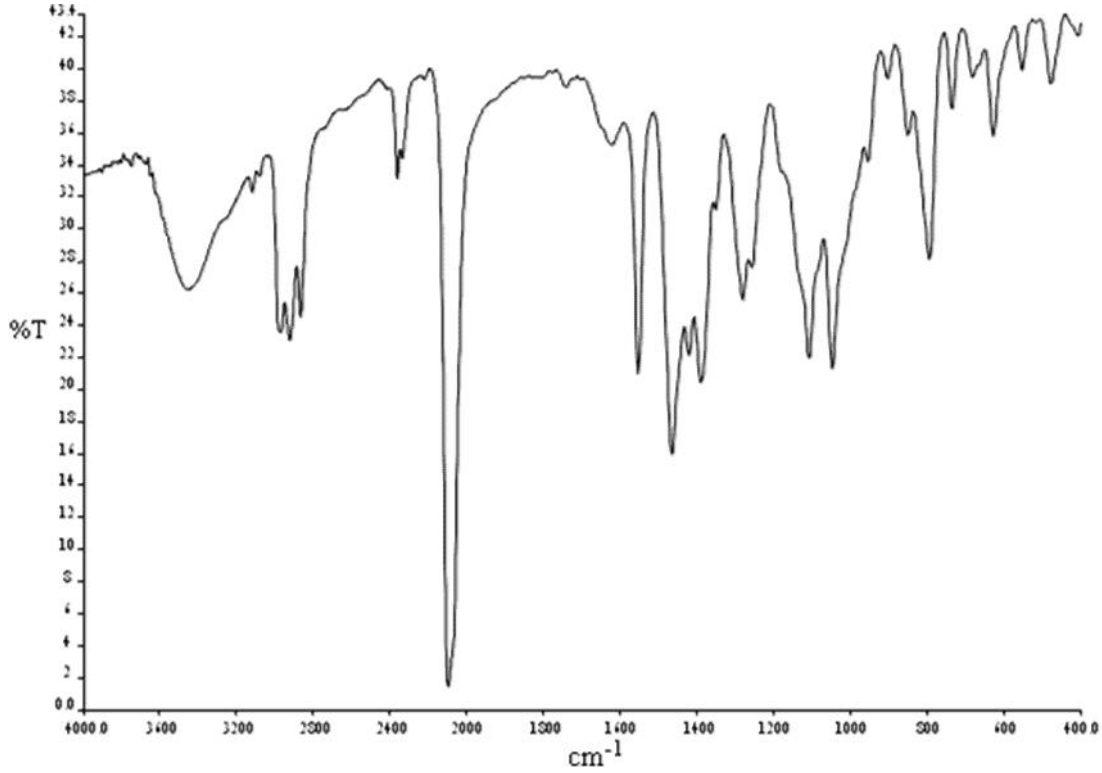

Fig.2.5. IR spectrum of [Ni(dbdmp)$(NCS)_2$] **(1)**.

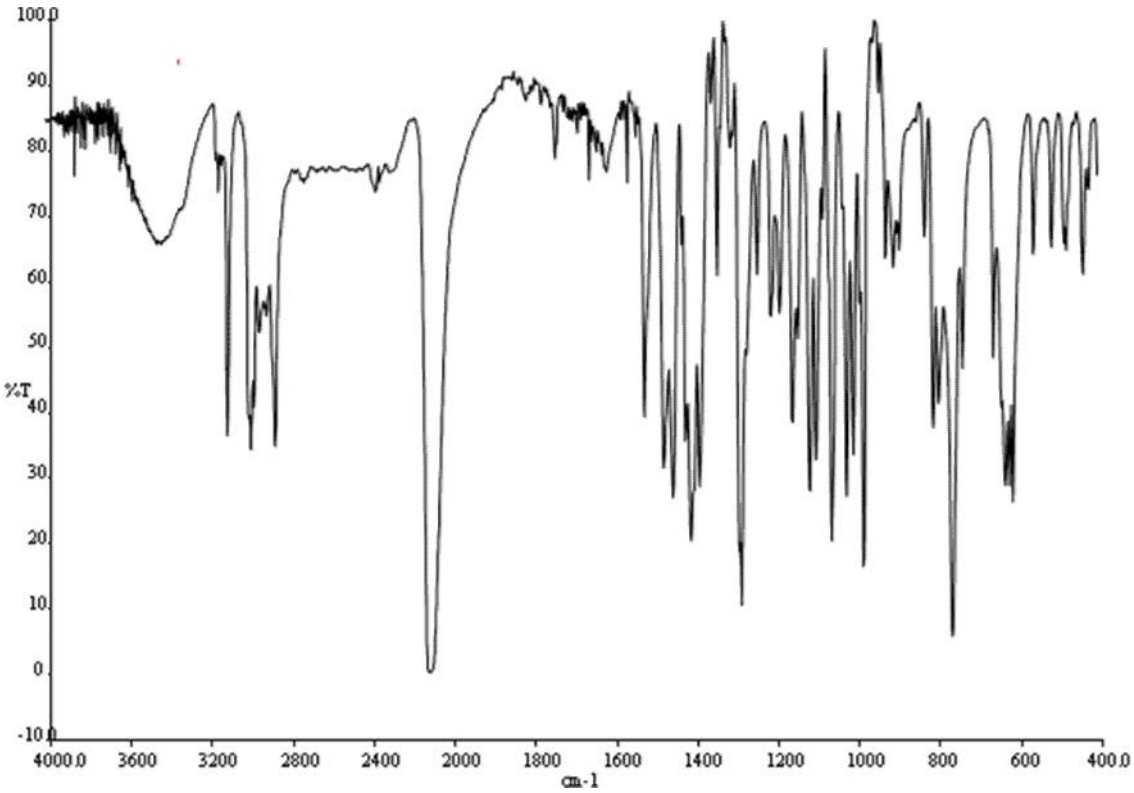

Fig.2.6. IR spectrum of [Ni(dbp)$(NCS)_2$] **(2)**.

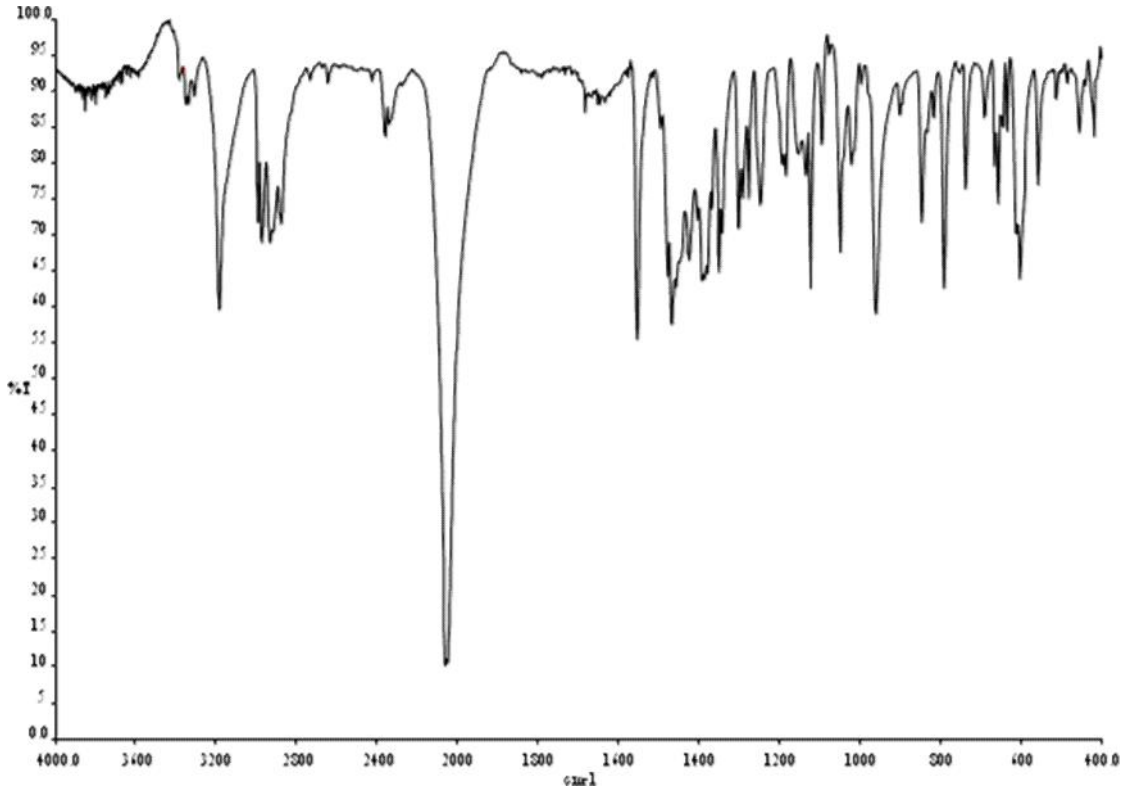

Fig.2.7. IR spectrum of $[Ni_2(L'_1)_2(N_3)_2(\mu\text{-}N_3)_2]$ **(3)**.

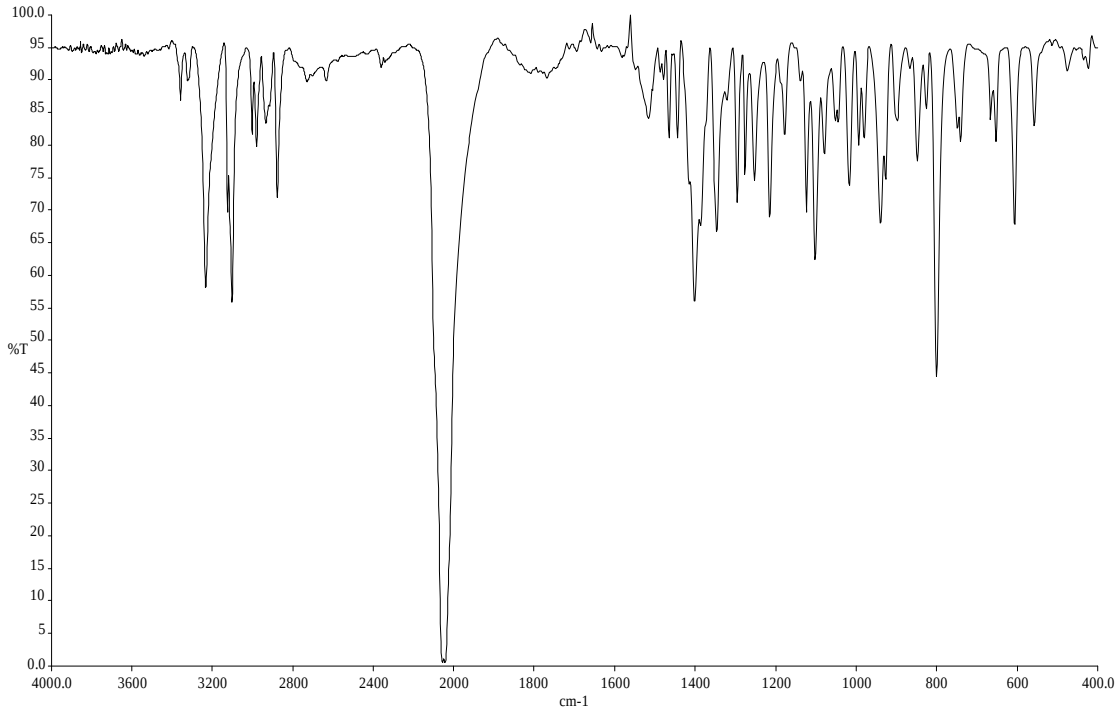

Fig.2.8. IR spectrum of $[Ni_2(L'_2)_2(N_3)_2(\mu\text{-}N_3)_2]$ **(4)**.

2.4.3.2. ^{1}H NMR and ^{13}C NMR Spectra of Ligands

The ^{1}H NMR spectra of ligands dbdmp and dbp are in good agreement with the proposed structures of the ligands. The ^{1}H NMR spectrum of ligand dbdmp [Fig.2.9] shows peak at 2.188-2.198 δ ppm which confirm the presence of four methyl group of pyrazole ring. The triplet and quartet appear at 0.919-0.955 and 2.397-2.432 δ ppm confirms the presence of CH_2-CH_3 group of ethylenediamine moity. Two triplets appear at 2.312-2.349 and 2.734-2.771 δ ppm confirm the presence of two ethyl group of ethylenediamine. A singlet appear at 4.918 δ ppm confirm the presence of -CH_2- which is connected with pyrazole and ethylenediamine moiety. The aromatic protons of pyrazole ring appear at 5.822 δ ppm.

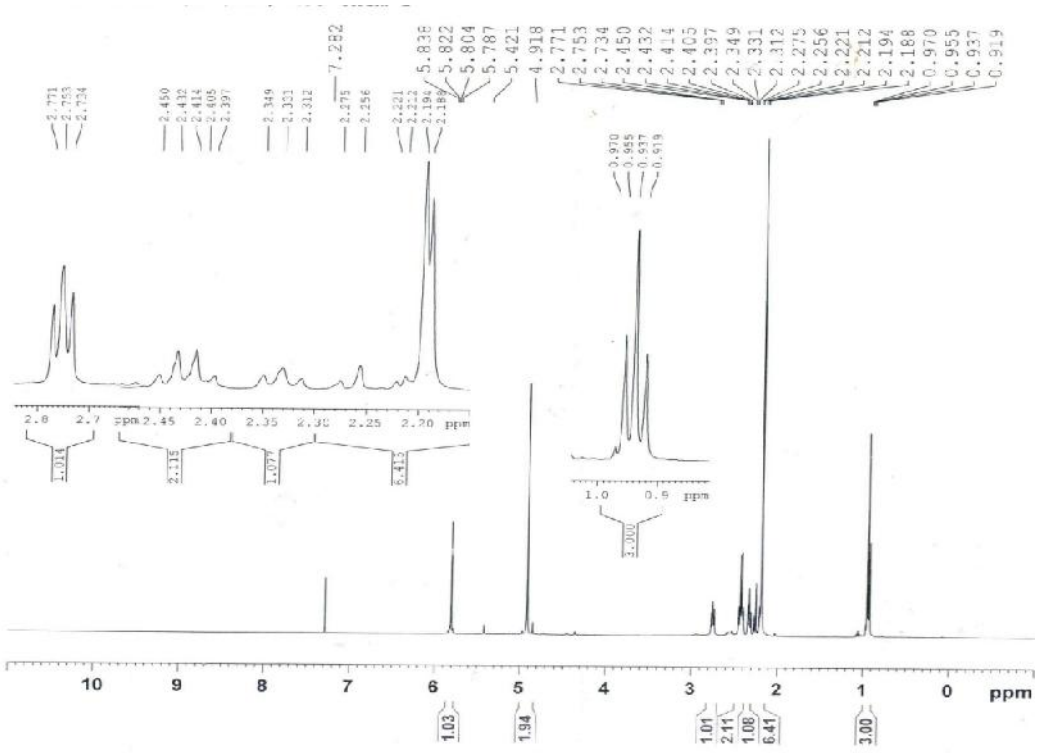

Fig.2.9. ^{1}H NMR spectrum of *N*,*N*-diethyl- *N′*,*N′*-bis((3,5-dimethyl-*1H*-pyrazol-1-yl)methyl)ethane -1,2-diamine (dbdmp).

In the ^{13}C NMR spectrum of ligand dbdmp [Fig.2.10], 10 singnals are observed which are corresponds to the presence of 10 carbons with different chemical environment. The spectrum shows three peak at 10.86, 11.40, 13.41 δ ppm for methyl carbons of pyrazole group and ethyl group. Three peaks at 46.84, 47.03 and 50.45 δ ppm are appeared due to methylene carbons of ethyl group and ethylenediamine. A peak at 65.70 δ ppm is due to methylene group which is connected with pyrazole and ethylenediamine moiety. In the spectrum, three peaks at 105.75, 139.60, and 147.43 δ ppm are corresponds to C3, C2 and C4 of pyrazole ring.

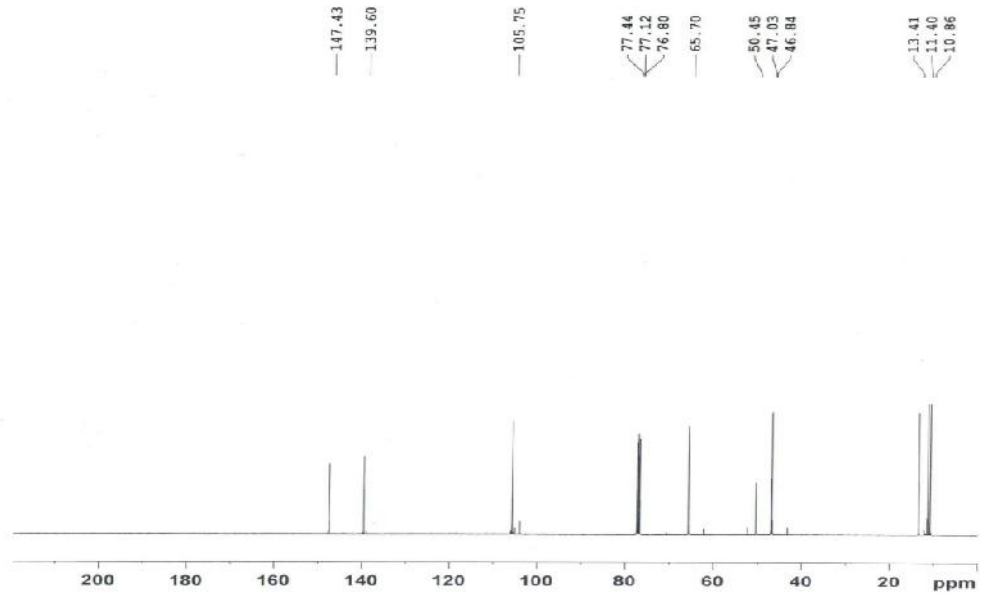

Fig.2.10. ^{13}C NMR spectrum of *N*,*N*-diethyl-*N'*,*N'*-bis((3,5-dimethyl-*1H*-pyrazol-1-yl)methyl)ethane -1,2-diamine (dbdmp).

In the ^{1}H NMR spectra of ligand dbp [Fig.2.11], triplet and quartet appear at 0.989-1.025 and 2.490-2.536 δ ppm confirms the presence of CH_2-CH_3 group of ethylenediamine moiety. The quartet of CH_2-CH_3 group is merged with the triplet of ethylenediamine's triplet protons which is observed at 2.536-2.573 δ ppm and another triplet is observed at 2.799-2.833 δ ppm. A singlet of -CH_2- group which is connected with pyrazole and ethylenediamine moiety is observed at 5.079 δ ppm confirm the formation of ligand dbp. A triplet and doublet of pyrazole ring's proton appear at 6.294-6.304 δ ppm and 7.554-7.619 δ ppm.

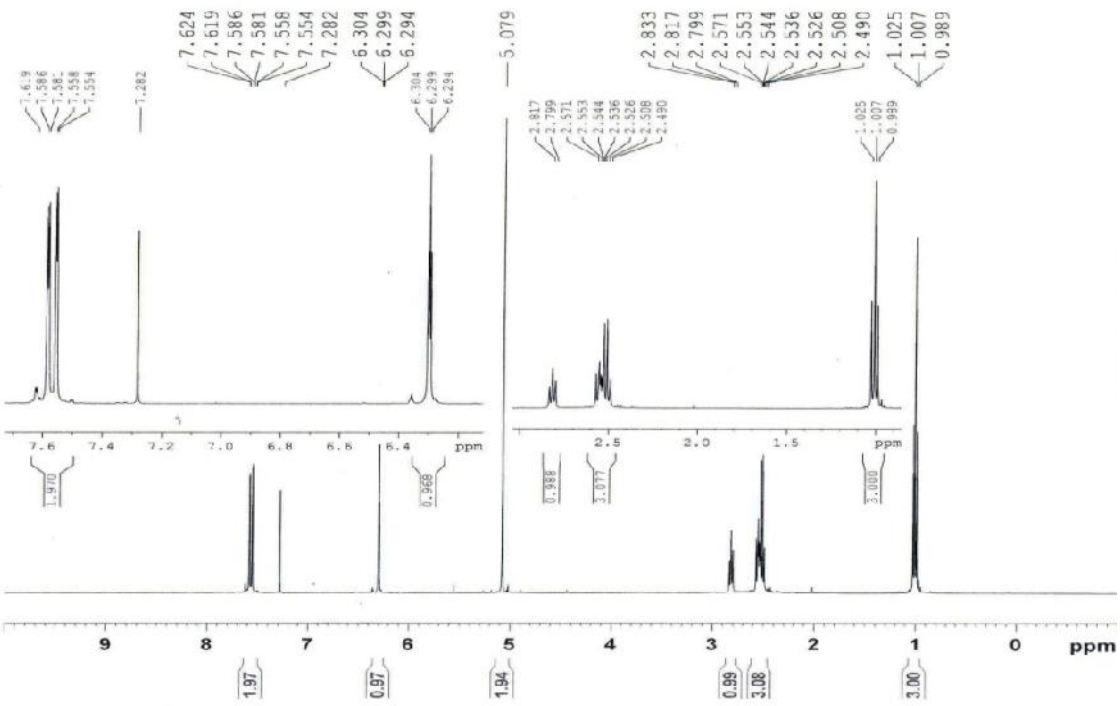

Fig.2.11. ^{1}H NMR spectrum of *N*,*N*-bis((*1H*-pyrazol-1-yl)methyl)-*N′*,*N′*-diethyl ethane-1,2-diamine (dbp).

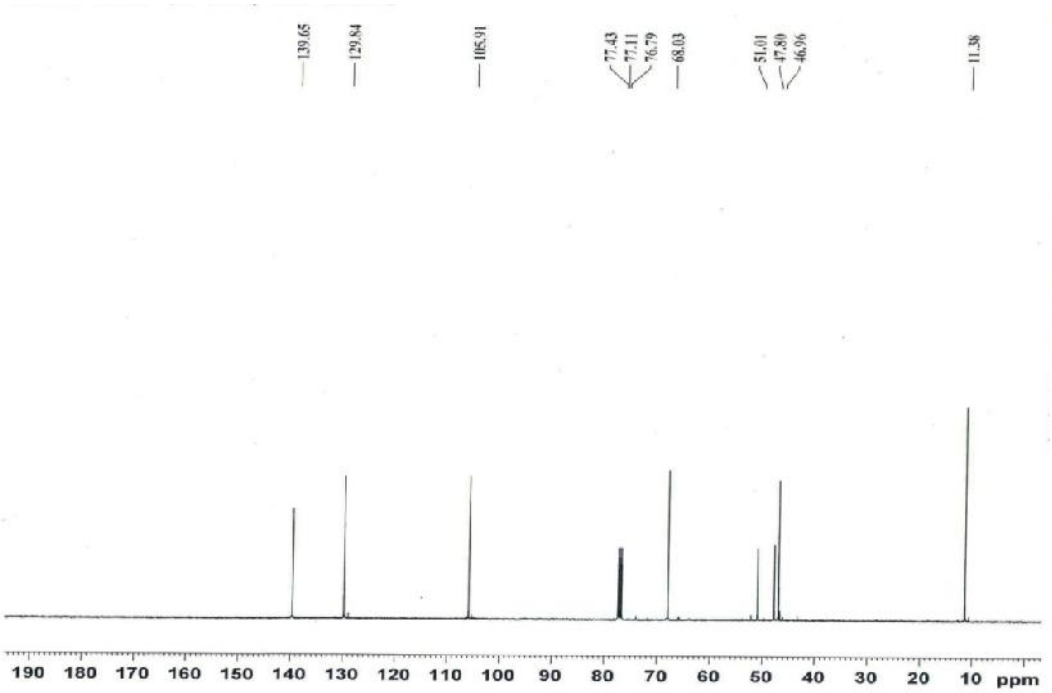

Fig.2.12. ^{13}C NMR spectrum of *N*,*N*-bis((*1H*-pyrazol-1-yl)methyl)-*N′*,*N′*-diethyl ethane-1,2-diamine (dbp).

In the ^{13}C NMR spectrum of ligand dbp [Fig.2.12], eight signals are observed which are corresponds to the presence of eight carbons with different chemical environment. The spectrum shows a peak at 11.38 δ ppm for methyl carbon of ethyl group. Three peaks at 46.96, 47.80 and 51.01 δ ppm are due to methylene carbons of ethyl group and ethylene diamine. A peak at 68.03 δ ppm is due to methylene group which is connected with pyrazole and ethylenediamine moiety. In the spectrum, three peaks at 105.91, 129.84, and 139.65 δ ppm are due to C2, C1 and C3 of pyrazole ring.

2.4.3.3. Electronic Spectra and Magnetic Properties of Complexes 1 and 2

The electronic spectra of complexes **1** and **2** in acetonitrile solution [Fig.2.13] show two absorption bands at ~ 672 and ~ 417 nm and these are attributed to d-d transition or metal-to-ligand charge transfer transition. Spectral bands below 400 nm are due to intraligand charge transfer. Room temperature magnetic susceptibilities of complexes **1** and **2** show two electrons paramagnetism (μ_{eff} ~ 2.88 BM) indicating octahedral geometry of the complexes.

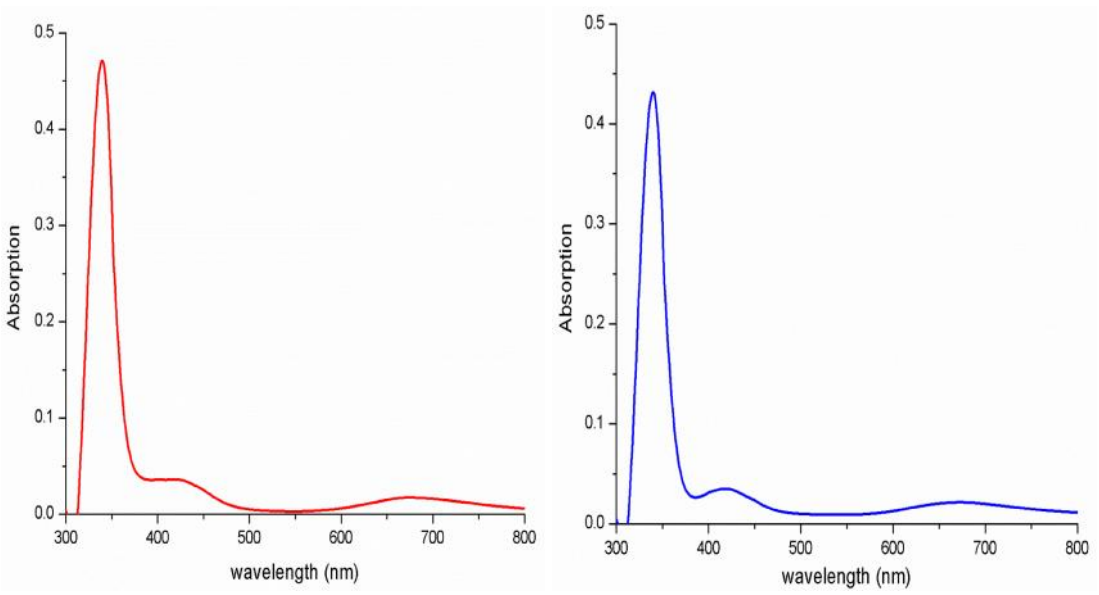

(1) **(2)**

Fig.2.13. Electronic spectra of [Ni(dbdmp)$(NCS)_2$] **(1)** and [Ni(dbp)$(NCS)_2$] **(2)**.

2.4.4. Magnetic Properties of Complexes 3 and 4

The magnetic properties of complexes **3** and **4** as $\chi_M T$ *vs* T plot (χ_M is the molar magnetic susceptibility for two Ni^{II} ions) are shown in Fig. 14. The value of $\chi_M T$ at 300 K is 2.5 $cm^3mol^{-1}K$ for **3** and 2.7 $cm^3mol^{-1}K$ for **4** and which is as expected for two magnetically spin triplets ($g > 2.00$). Starting from room temperature $\chi_M T$ values increase to 3.44 at 15 K for **3** and to 3.63 at 20 K for **4** and below this temperature $\chi_M T$ decreases quickly to 2.81 and 3.13 cm^3mol^{-1} K respectability at 2 K.

This feature indicates the presence of ferromagnetic exchange interaction within the Ni(II) dimer together with the presence of both D (a zero field splitting of the resulting S = 2 spin ground state) and z'J' (intermolecular antiferromagnetic interactions). Both D and J' are strongly correlated and show same results at low temperature. Thus, it was not possible to separate them in any attempt to fit the experimental data [47]. So two different approaches have been used to fit the experimental data: either considering the z'J' parameter (by means of molecular-field approximation) [48] or the D (zero-field-splitting parameter) by the full-diagonalization MAGPACK program that uses the $-2J(S_1.S_2)$ Hamiltonian [49].

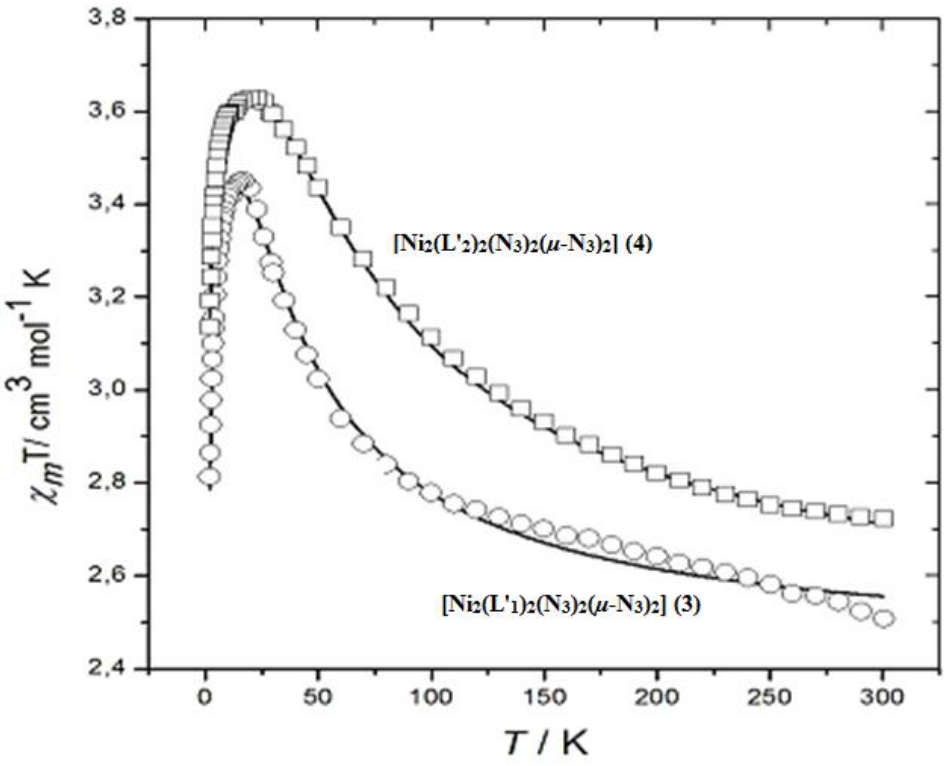

Fig.2.14. Temperature Dependence of the magnetic moment ($\chi_M T$ *vs* T*)* of the complexes **3** and **4**. The solid lines represent the best fit of the data.

The best-fit parameters obtained with the first approach is J = 18.61 ± 0.5 cm^{-1}, J' = -0.21 cm^{-1} , g = 2.20 ± 0.01 and R = 2.7 x 10^{-4} for **3** and J = 31.87 ± 0.4 cm^{-1}, J' = -0.12 cm^{-1}, g = 2.22 ± 0.01 and R = 3.6 x 10^{-4} for **4.** Slightly different J values were obtained by using the D parameter. In this case, the best-fit parameters obtained are J = 24.12 ± 0.5 cm^{-1}, D = 3.9 ± 0.6 cm^{-1}, g = 2.15 ± 0.01 and R = 9.8 x 10^{-3} for **3** and J = 39.34 ± 0.5 cm^{-1}, D = 3.02 ± 0.5 cm^{-1}, g = 2.19 ± 0.01 and R = 3.2 x 10^{-4} for **4.** As occurs through this calculation, the D parameter is overestimated, because the logical J' parameter is not considered. As a consequence, we can postulate that the best model is the first one and consequently the J value is closer to 19 cm^{-1} for **3** and 32 cm^{-2} for **4**; J' could be of the order of -0.2 cm^{-1} and D will be, likely, less than 4 cm^{-1} (the standard value for isolated nickel(II) complexes is close to 6 cm^{-1}) [49].

The J values are perfectly correlated with those values reported in the literature for similar complexes. Indeed, all these complexes show ferromagnetic coupling. The number of Ni^{2+} dinuclear complexes reported with two EO azido bridging ligands has increased considerably over the past 15 years. The formula of the core is $[Ni_2(\mu_{1,1}\text{-}N_3)_2]^{2+}$. A review of these (and other) complexes was made by Ribas et al in 1999 [1]. J values lie between 20 cm^{-1} and 70 cm^{-1} approximately. All dinuclear complexes have a Ni-N-Ni angle close to 100º.

Ruiz et al carried out a theoretical study of these bis(μ-azido) complexes. The interaction is predicted to be ferromagnetic or all range of Ni-N-Ni angles, with J increasing upon increasing this angle, yielding a maximum at 104º approximately. They also studied the influence of the out-of-plane displacement of the azido group, being its effect on the exchange coupling very small. The influence of the Ni-N distance was also investigated, indicating a poorer ferromagnetic coupling as the bond distance increases, though in this case, the experimental data does not seem to follow the predicted trend [49]. The J value of both compound are included in the range for all reported values [51], which seems consistent with the Ni-N-Ni angle (99º).

2.5. Conclusion

In this chapter, we have reported synthesis and characterization of two new ligands *N*,*N*-diethyl-*N*′,*N*′-bis((3,5-dimethyl-*1H*-pyrazol-1-yl)methyl)ethane-1,2-diamine (dbdmp), *N*,*N*-bis((*1H*-pyrazol-1-yl)methyl)-*N*′,*N*′-diethylethane-1,2-diamine (dbp), two mononuclear octahedral nickel(II) complexes [Ni(dbdmp)$(NCS)_2$] (**1**) and [Ni(dbp)$(NCS)_2$] (**2**) and two azido bridged binuclear nickel(II) complexes $[Ni_2(L'_1)_2(N_3)_2(\mu\text{-}N_3)_2]$ (**3**) and $[Ni_2(L'_2)_2(N_3)_2(\mu\text{-}N_3)_2]$ (**4**). Crystal structures of the complexes **1**, **2**, **3** and **4** show that complex **1** and **2** are mononuclear with octahedral geometry and complexes **3** and **4** are double end-on azido bridged octahedral binuclear nickel(II) complexes. L'_1 and L'_2 are formed from ligands dbdmp and dbp during the reaction. Both the nickel complexes **3** and **4** show predominantly ferromagnetic interaction at variable temperature magnetic studies with the *J* values 19 and 32 cm^{-1} respectively. Change of coordination sites of the ligand from pyridine to *N*,*N*-diethylethylenediamine, coordination mode of azide changes from end-to-end to end-on in the bridged complexes.

2.6. References:

1. J. Ribas, A. Escuer, M. Montfort, R. Vicente, R. Cortés, L. Lezama, T. Rojo, *Coord. Chem. Rev.* 193-195 (1999) 1027.

2. J. Ribas, M. Monfort, C. Diaz, C. Basto, X. Solans, *Inorg. Chem.* 32 (1993) 3557.

3. J. Ribas, M. Monfort, B. K. Ghosh, R. Cortes, X. Solans, M. Font-Bardia, *Inorg. Chem.* 35 (1996) 864.

4. M. A. Goher, A. Escuer, F. A. Mautner, N. A. Al-Salem, *Polyhedron* 21 (2002) 1876.

5. Z-H. Zhang, X-H. Bu, Z-H. Ma, W-M. Bu, Y. Tang, Q-H. Zhao, *Polyhedron* 19 (2000) 1559.

6. G-F. Liu, Z. G. Ren, H-X. Li, Y. Chen, Q-H. Li, Y. Zhang, J-P. *Lang, Eur. J. Inorg. Chem.* 35 (2007) 5511.

7. S. S. Tandon, S. D. Bunge, R. Rakosi, Z. Xu, L. K. Thompson, *J. Chem. Soc., Dalton Trans.* 33 (2009) 6536.

8. M. Monfort, I. Resino, J. Ribas, X. Solans, M. Font-Bardia, H. Stockli- Evans, *New J. Chem.* 11 (2002) 1601.

9. T. K Maji, P. S. Mukherjee, G. Mostafa, T. Mallah, J. Cano-Boquera, N. R. Caudhury, *Chem Commun.* 11 (2001) 1012.

10. P. S. Mukherjee, S. Dalai, G. Mustafa, T-H. Lu, E. Rentschler, N. R. Raychaudhury, *New J. Chem.* 9 (2001) 120.

11. F. D. Biani, E. Ruiz, J. Cano, J. J. Novoa, S. Alvarez, *Inorg. Chem.* 39 (2000) 3221.

12. X-T. Wang, X-H. Wang, Z-M. Wang, S. Gao, *Inorg. Chem.* 48 (2009) 1301.

13. P. Chaudhuri, R. Wagner, S. Khanra, T. Weyhermuller, J. Chem. Soc., *Dalton Trans.* (2006) 4962.

14. P. Chaudhuri, T. Weyhermuller, E. Bill, K. Weighardt, *Inorg. Chim. Acta* 252 (1996) 195.

15. L. Li, D. Liao, Z. Jiang, P. Monesca Rey, *Inorg. Chem.* 45 (2006) 7665.

16. S. Konar, S. Saha, T. Mallah, K-I. Okamoto, *Inorg. Chem.* 43 (2004) 840.

17. Y. Song, C. Massera, O. Roubeau, P. Gamez, A. Maria, A. M. M. Lanfredi, J. Reedijk, *Inorg. Chem.* 43 (2004) 6842.

18. T. K. Karmakar, S. K. Chandra, J. Ribas, G. Mostafa, T. H. Lu, B. K. Ghosh, *Chem Commun.* (2002) 2364.

19. F-C. Liu, J-P. Zhao, B-W. Hu, Y-F. Zeng, J. Ribas, X-H. Bu, *J. Chem. Soc. Dalton Trans.*, (2010) 1185.

20. S-Q. Bai, E-Q. Gao, Z. He, C-J. Fang, C-H. Yau, *New J. Chem.* 29 (2005) 935.

21. Z. X. Miao, M. X. Li, M. Shao, H. J. Liu, *Inorg. Chem. Commun.* 10 (2007) 1117.

22. S. Koner, S. Saha, K-I. Okamoto, J-P. Tuchagues, *Inorg. Chem.*, 42 (2003) 4668.

23. X. Y. Song, W. Li, L. C. Li, D. X. Liao, Z. H. Jiang, *Inorg. Chem. Commun.* 10 (2007) 567.

24. S. S. Massoud, L-Le Quan, K. Gatterer, J. H. Albering, R. C. Fischer, F. A. Mautner, *Polyhedron* 31 (2012) 601.

25. M. Zala, E. Suresh, S. B. Kumar, *J. Coord. Chem.* 64 (2011) 438.

26. T. K. Karmakar, M. Ghosh, M. Fleck, G. Pilet, D. Bandyopadhyay, *J. Coord. Chem.* 65 (2012) 2612.

27. A. Jana, S. Konar, K. Das, S. Ray, J. A. Golen, A. L. Rheingold, L. M. Carrellaa, E. Rentschler, T. K. Mondal, S. K. Kar, *Polyhedron* 38 (2012) 258.

28. S. Sain, S. Bid, A. Usman, H.-K. Fun, G. Aromi, X. Solans, S. K. Chandra, *Inorg. Chim. Acta* 358 (2005) 3362.

29. S. Sarkar, A. Mondal, M. Salah, E. Fallah, J. Ribas, D. Chopra, H. S.- Evans, K. K. Rajak, *Polyhedron* 25 (2006) 25.

30. R. Shridhar, P. T. Perumal, S. Etti, G. Shanmugam, M. N. Ponnuswamy, V. Prabavathy, R. N. Mathivanna, *Bioorg. Med. Chem. Lett.* 14 (2004) 6035.

31. A. K. Jain, S. M. Moore, K. Yamaguchi, T. E. Eling, S. J. Back, *J. Pharmacol Exp. Ther.* 311 (2004) 885.

32. A. Escuer, R. Vicente, J. Ribas, M. S. El Fallah, X. Solans, M. Font-Bardıa, *Inorg. Chem.* 32 (1993) 3727.

33. M. Monfort, I. Resino, J. Ribas, X. Solans, M. Font-Bardıa, *New J. Chem.* 25 (2001) 1577.

34. M.-F. Charlot, O. Kahn, M. Chaillet, C. Larrieu, *J. Am. Chem. Soc.* 108 (1986) 2574.

35. L. K. Thompson, S. S. Tandon, M. E. Manuel, *Inorg. Chem.* 34 (1995) 2356.

36. J. Ribas, M. Monfort, B. K. Ghosh, X. Solans, *Angew Chem. Int. Ed. Engl.*, 33 (1994) 2087.

37. W. L. Driessen, *Recl. Trav. Chim. Pays-Bas.* 101 (1982) 441.

38. G. M. Sheldrick. SAINT, 5.1 ed. *Siemens Industrial Automation Inc., Madison, WI* (1995).

39. G. M. Sheldrick. SADABS, *Empirical Absorption Correction Program, University of Gottingen, Gottingen, Germany* (1997).

40. G. M. Sheldrick. *SHELXTL Reference Manual (Version 5.1), Bruker AXS, Madison, WI* (1997).

41. G. M. Sheldrick. SHELXL-97: *Program for Crystal Structure Refinement, University of Gottingen, Gottingen* (1997).

42. S. Bhattacharyya, T. J. R. Weakley, M. Chaudhury, *Inorg. Chem.* 38 (1999) 5453.

43. S. Bhattacharyya, T. J. R. Weakley, M. Chaudhury, *Inorg. Chem.* 38 (1999) 633.

44. M. R. Malachowski, A. S. Kasto, M. E. Adams, A. L. Rheingold, L. N. Zakharov, L. D. Margerum, M. Greaney, *Polyhedron* 28 (2009) 393.

45. H. Yang, Y. Tang, Z-F. Shang, X-L. Han, Z-H. Zhang, *Polyhedron* 28 (2009) 3491.

46. M. Zala, S. B. Kumar, E. Suresh, J. Ribas, *Trans. Met. Chem.* 35 (2010) 757.

47. A. P. Ginsberg, R. L. Martin, R. W. Brookes, R. C. Sherwood, *Inorg. Chem.* 11 (1972) 2884.

48. O. Kahn, *Molecular Magnetism, VCH, New York* (1993).

49. MAGPACK Program., J. J. Borrás-Almenar, J. M. Clemente–Juan, E. Coronado, B. S. Tsukerblat, *Inorg. Chem.* 38 (1999) 6081.

50. E. Ruiz, J. Cano, S. Alvarez, P. Alemany, *J. Am. Chem. Soc.* 120 (1998) 11122.

51. R. Boca, *Coord. Chem. Rev.* 248 (2004) 757.